Bio-Inspired Cross-Layer Communication and Coordination in Sensor and Vehicular Actor Networks

Baris Atakan, *Member, IEEE*, and Ozgur B. Akan, *Senior Member, IEEE*

***Abstract*—In this paper, based on *the prey model in foraging theory*, the BIO-inspired Cross-layer (BIOX) communication and coordination protocol is introduced for wireless sensor and actor networks (WSANs). BIOX permits each sensor node to autonomously determine its next-hop selection and channel access strategy using bio-inspired *next-hop selection* and *channel access profitability measures*. Based on these profitability measures, BIOX provides optimal performance in energy-efficient and reliable sensor–actor communication. Furthermore, using *task allocation profitability measure*, BIOX also guarantees stable allocation of available tasks in a way that each task is accomplished by an actor node within a bounded time delay. Performance evaluations reveal that BIOX significantly prolongs the network lifetime while providing highly reliable sensor–actor communication and effective task allocation for actor nodes.**

***Index Terms*—Bio-inspired communication, foraging theory, wireless sensor and vehicular actor networks.**

I. Introduction

WIRELESS sensor and actor networks (WSANs) consist of a number of communicating sensor and vehicular actor nodes for performing distributed sensing and acting tasks [1]. Energy-efficient, timely, and reliable sensor–actor communication are the main challenges for the realization of WSANs. Furthermore, cooperative control of actor nodes is also essential in realizing an effective task allocation among the actor nodes. In the literature, there are many studies on energy-efficient communication protocols for wireless sensor networks (WSNs) and WSANs [2]–[6]. However, the major common drawback of these proposals is the lack of autonomy in the operations of the network nodes. To provide the autonomous network operations for WSANs, in this paper, inspired by the prey model in foraging theory, we introduce the BIO-inspired cross-layer (BIOX) communication and coordination protocol for WSANs. BIOX provides three different nature-inspired profitability measures called *next-hop selection*, *channel access*, and *task allocation profitability* for the sensor and actor nodes. The aim of these measures is to control the rate of gain in energy efficiency, reliability, and stability of the network operations. Using the next-hop selection profitability measure, each sensor node selects its next hop node in an energy-efficient way. Sensor nodes also schedule their transmissions by means of channel access profitability to provide a reliable sensor–actor communication. Based on the task allocation profitability, each actor node selects and accomplishes a set of tasks. BIOX is a fully autonomous algorithm and produces an optimal performance in prolonging network lifetime and reliable sensor–actor communication. Moreover, it also provides stable allocation of available tasks in a way that each task is accomplished within a bounded time delay by the most appropriate actor node. The BIOX protocol can be applicable to any data type observed in the sensed field. For example, if sensor nodes sense the humidity level of an agricultural field, these levels are first sampled, and data packets are formed using these samples to transmit to actor nodes. Here, we note that, aside from the prey model, the marginal value theorem in behavioral ecology and biological division of labor phenomenon can also be adopted to develop autonomous communication and coordination techniques for WSANs and WSNs, as proposed in [7]–[9]. These works are promising in showing how biological principles can be applied to WSANs and WSNs to develop efficient communication and coordination schemes.

The remainder of this paper is organized as follows: In Section II, we introduce the design principles of BIOX. In Section III, we derive a BIOX communication model. The task allocation model of actor nodes is introduced in Section IV. In Section V, we present the BIOX protocol operation. In Section VI, performance evaluations are presented, and concluding remarks are given in Section VII.

II. Bio-Inspired Cross-Layer Protocol Design Principles

In this section, we first describe the network model and assumptions, and formulate the cross-layer optimization problem. Then, we review a *prey model in foraging theory*, based on which we develop a BIOX communication model for WSANs.

Manuscript received September 6, 2011; revised January 17, 2012; accepted February 13, 2012. Date of publication March 13, 2012; date of current version June 12, 2012. The review of this paper was coordinated by Prof. A. Jamalipour.

B. Atakan was with the Next-Generation and Wireless Communications Laboratory, Department of Electrical and Electronics Engineering, Koç University, Istanbul 34450, Turkey. He is now with Broadband and Wireless Networking Laboratory, School of Electrical and Computer Engineering, Georgia Institute of Technology, Atlanta (e-mail: batakan@ku.edu.tr; akan@ku.edu.tr).

O. B. Akan is with the Next-Generation and Wireless Communications Laboratory, Department of Electrical and Electronics Engineering, Koç University, Istanbul 34450, Turkey.

Color versions of one or more of the figures in this paper are available online at http://ieeexplore.ieee.org.

Digital Object Identifier 10.1109/TVT.2012.2190831

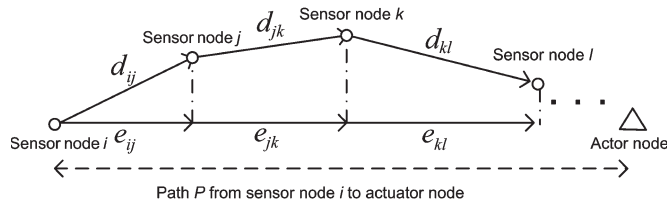

Fig. 1. Data path from sensor node i to the actor node. Hop distances $(d_{ij}\ \forall i,j)$ and effective hop distances $(e_{ij}\ \forall i,j)$ are shown in the path.

A. Network Model and Problem Formulation

We consider a network architecture in which N sensor nodes are deployed in an environment. Sensor nodes separately detect and transmit event information to M vehicular actor nodes. Each source node samples the event signal and transmits the generated data frames with an average reporting frequency, i.e., f (in frames per second). Sensor nodes participating in data transmission and/or reception are called active sensor nodes.

The wireless channel is assumed to be shared in fixed-duration time slots, which are, in turn, captured by sensor nodes in order not to interfere with each other. Using a time slot, a sensor node either transmits or receives a data frame. The duration of a time slot consists of two intervals named frame transmission and acknowledgment (ACK) interval. In the frame transmission interval, sensor nodes transmit the frame header and payload. The frame header includes the identity (ID) number of the source node that initially generates the current packet. This enables each sensor node to infer how many source nodes it serves to route toward the actor node.

Sensor nodes initially have the same level of energy, i.e., E, and each sensor node i periodically measures its residual energy level E_i. Sensor node i is assumed to consume $H(d_{ij})$ joule of energy to receive and transmit a bit to sensor node j. d_{ij} denotes the Euclidean distance between sensor node i and sensor node j [11]. For a sensor node, transmission cost, i.e., the level of dissipated energy, heavily depends on its hop distance (d_{ij}). Furthermore, overall energy consumption along a path is also affected by the effective hop distances (e_{ij}), which are the absolute Euclidean distance toward the destination actor by a hop, as shown in Fig. 1. The total energy consumption throughout path P in Fig. 1, i.e., C_P, is given as $C_P = \sum_{(i,j)\in P} H(d_{ij})$, where $(i,j) \in P$ means the directed arc (i,j) between sensor node i and j is on path P. Furthermore, the Euclidean distance D_P of path P can also be given by adding the effective hop distances (e_{ij}) as $D_P = \sum_{(i,j)\in P} e_{ij}$. Using the log-sum inequality, C_P and D_P can also be incorporated to derive an upper bound for C_P as

$$\sum_{(i,j)\in P} H(d_{ij}) \log \frac{H(d_{ij})}{e_{ij}} \geq \left(\sum_{(i,j)\in P} H(d_{ij}) \right) \log \frac{C_P}{D_P}. \quad (1)$$

By modifying (1), it can also be rewritten as

$$\log D_P + \frac{\sum_{(i,j)\in P} H(d_{ij}) \log \frac{H(d_{ij})}{e_{ij}}}{\sum_{(i,j)\in P} H(d_{ij})} \geq \log C_P. \quad (2)$$

Assume that $H(d_{ij})/e_{ij}$ is a random variable. Then, its expected value, i.e., $\gamma_P = E[H(d_{ij})/e_{ij}]$, can be expressed as

$$\gamma_P = \sum_{(i,j)\in P} \sum_{j\in n_i} p_{ij} \frac{H(d_{ij})}{e_{ij}} \quad (3)$$

where p_{ij} is the probability that sensor node i transmits to sensor node j. n_i is the set including all node ID numbers in the communication range of sensor node i. By replacing $H(d_{ij})/e_{ij}$ with $\gamma_P = E[H(d_{ij})/e_{ij}]$, (2) can also be approximated as

$$\log D_P + \frac{\log \gamma_P \sum_{(i,j)\in P} H(d_{ij})}{\sum_{(i,j)\in P} H(d_{ij})} \geq \log C_P. \quad (4)$$

By further simplifying (4), an upper bound for C_P can be found as

$$\log D_P + \log \gamma_P \geq \log C_P$$
$$D_P \gamma_P \geq C_P. \quad (5)$$

In addition to the minimization of C_P, it is also imperative to provide balanced energy consumption over the network nodes to maximize the network lifetime. For this aim, sensor nodes having high residual energy should be mostly activated. Therefore, along path P, if sensor node j has a high level of residual energy, each sensor node i maximizes p_{ij} to mostly transmit to sensor node j. This strategy clearly maximizes the expected total residual energy of active sensor nodes, i.e., β_P, that can be expressed as

$$\beta_P = \sum_{(i,j)\in P} \sum_{j\in n_i} p_{ij} E_j \quad (6)$$

where E_j is the residual energy of sensor node j. Briefly, the maximization of (6) allows the sensor nodes with high level of residual energy to be activated, which eventually provides balanced energy consumption throughout the network.

1) Cross-Layer Optimization Problem: Based on the aforementioned definitions and notations, the cross-layer optimization problem to ensure energy-efficient and reliable sensor–actor communication can be given as follows.

1) For energy optimization, it is imperative for each path P to perform the following:
   a) Minimize the energy consumption of the active sensor nodes by minimizing γ_P in (3).
   b) Mostly activate the sensor nodes having high residual energies by maximizing β_P in (6). These objectives can be achieved by easily maximizing the ratio J_P of β_P to γ_P, i.e., $J_P = \beta_P/\gamma_P$.
2) For reliable sensor–actor communication, the average frame transmission rate of sensor node i, i.e., η_i, must be greater than the average frame rate, i.e., $s_i f$, transmitted to sensor node i. This clearly entails satisfying a condition, i.e., $s_i f < \eta_i\ \forall i$ to prevent possible congestion and packet losses on sensor node i. Using the aforementioned

requirements, the cross-layer optimization problem can be formulated as follows:

$$\text{maximize} \quad J_P \quad \forall P \tag{7}$$
$$\text{subject to} \quad s_i f < \eta_i \quad \forall i. \tag{8}$$

Next, inspired by a prey model in foraging theory, we propose an optimal solution for the cross-layer optimization problem formulated in (7) and (8). To this end, we first review the prey model in foraging theory.

B. Prey Model in Foraging Theory

Foraging theory is a field in behavioral ecology to mathematically describe models based on which the foraging animals search for nutrients and choose which ones to consume [12]–[14]. The fundamental claim in foraging theory is that animals search for and obtain nutrients by maximizing their energy intake E per unit time T. This strategy is mathematically characterized by the maximization of an objective function of (E/T) [14]. One of the classical foraging models is the prey model. The prey model describes a forager searching for different prey types in a particular environment. Each prey holds a certain energy intake. The forager must search for and recognize a prey for the energy intake. Once it encounters and recognizes a prey, it decides whether to handle it [12]. Assume that there are k different types of prey in the environment. t_i is the expected time required to handle prey type i, and ν_i is the expected amount of energy intake obtained from handling prey i. The average rate of encounter with prey i is λ_i. p_i is the probability that prey type i is handled once it is found and recognized. Hence, the average rate of gain of a forager, i.e., J, can be defined as a ratio of the total expected energy intake to expected amount of time spent for searching and handling the prey types. Hence, J can be expressed as

$$J = \frac{\sum_{i=1}^{k} p_i \lambda_i \nu_i}{1 + \sum_{i=1}^{k} p_i \lambda_i t_i}. \tag{9}$$

The prey model allows a forager to maximize J by finding the optimal values of p_i $\forall i$. In particular, the prey model uses a zero-one rule to maximize J such a way that each forager separately decides which prey should be consumed by setting p_i either $p_i = 0$ or $p_i = 1$. In this paper, this mechanism is mainly adopted and used for an autonomous communication and coordination protocol for WSAN.

C. Inspiration From Prey Model

Here, to establish a bio-inspired communication and coordination model for WSAN, we consider sensor and actor nodes as forager. Similar to a forager searching for prey, each sensor node searches for the possible next hop node and available time slots to forward its packets toward an actor node. Each actor also searches for and performs available tasks associated with the event. Hence, for a sensor node, its possible next hop nodes and available time slots are considered as prey in the prey model. Available tasks are also considered as prey types that are searched and performed by the actor nodes. Based on these analogies, we define three profitability measures named as *the next-hop selection*, *channel access*, and *task allocation profitability*. Using the next-hop selection profitability, each sensor node selects its next hop node. Based on the channel access profitability, each sensor node determines its transmission strategy. Actor nodes use the task allocation profitability to share and perform the available tasks.

III. Bio-Inspired Cross-Layer Sensor–Actor Communication Model

In this section, we introduce the next-hop selection profitability and channel access profitability measures based on which sensor nodes select and access their next hops.

A. Next-Hop Selection Profitability

In the prey model, the rate of gain, i.e., J, in (9) is maximized by determining the optimal p_i values. Similarly, as given in the formulation of the cross-layer optimization problem in (7) and (8), J_P can be considered as a rate of gain of the next-hop selection process. J_P can also be maximized by determining the optimal p_{ij} values as follows:

Theorem 1: To find the optimal p_{ij} values that maximize J_P, a zero-one rule can be derived via the next-hop selection profitability measure θ_{ij} given by

$$\theta_{ij} = \frac{E_j e_{ij}}{H(d_{ij})} \qquad \forall i, j \tag{10}$$

where E_j is the residual energy of sensor node j. $H(d_{ij})$ denotes the energy consumed by sensor node i to receive and transmit a bit to sensor node j. e_{ij} is the effective hop distance between sensor node i and j, as shown in Fig. 1.

Proof: To find the optimal p_{ij}, J_P can be rewritten as

$$J_P = \frac{p_{ij} E_j + \delta_{ij}}{p_{ij} \frac{H(d_{ij})}{e_{ij}} + \kappa_{ij}} \tag{11}$$

where δ_{ij} and κ_{ij} are expressed as

$$\delta_{ij} = \sum_{\substack{(z,k)\in P \\ z\neq i}} \sum_{\substack{k\in n_z \\ k\neq j}} p_{zk} E_k \text{ and } \kappa_{ij} = \sum_{\substack{(z,k)\in P \\ z\neq i}} \sum_{\substack{k\in n_z \\ k\neq j}} p_{zk} \frac{H(d_{zk})}{e_{zk}}. \tag{12}$$

Then, J_P can be differentiated with respect to p_{ij} as

$$\frac{\partial J_P}{\partial p_{ij}} = \frac{E_j \kappa_{ij} - \frac{H(d_{ij})}{e_{ij}} \delta_{ij}}{\left(p_{ij} \frac{H(d_{ij})}{e_{ij}} + \kappa_{ij} \right)^2}. \tag{13}$$

By considering $\partial J_P / \partial p_{ij} = 0$, the optimal p_{ij} can be found as follows.

1) If $(E_j e_{ij}/H(d_{ij})) < (\delta_{ij}/\kappa_{ij})$, then the numerator of (13) is negative. In this case, J_P can be maximized by choosing the lowest possible p_{ij}.
2) Conversely, if $(E_j e_{ij}/H(d_{ij})) > (\delta_{ij}/\kappa_{ij})$, then the numerator is positive. In this case, J_P can be maximized by choosing the possible highest p_{ij}.

Since $0 \leq p_{ij} \leq 1$, the lowest and highest possible p_{ij} can be given as $p_{ij} = 0$ and $p_{ij} = 1$, respectively. Consequently, the selection of p_{ij} to maximize J_P leads to a zero-one rule

$$\begin{aligned} \textbf{set} \quad p_{ij} = 0, \quad \textbf{if} \quad \frac{E_j e_{ij}}{H(d_{ij})} < \frac{\delta_{ij}}{\kappa_{ij}} \\ \textbf{set} \quad p_{ij} = 1, \quad \textbf{if} \quad \frac{E_j e_{ij}}{H(d_{ij})} > \frac{\delta_{ij}}{\kappa_{ij}} \end{aligned} \tag{14}$$

where $(E_j e_{ij})/(H(d_{ij}))$ is the profitability measure, i.e., θ_{ij}, defined in (10). Hence, sensor node j is a possible next hop of sensor node i if $p_{ij} = 1$, and it is not if $p_{ij} = 0$. Since each sensor node i selects a single next hop node, it selects its next hop as one of its possible next hop nodes satisfying $(E_j e_{ij})/(H(d_{ij})) > (\delta_{ij})/(\kappa_{ij})$ with the maximum next-hop selection profitability $E_j e_{ij}/H(d_{ij})$. Such a next hop node can clearly maximize J_P by maximizing $(\partial J_P)/(\partial p_{ij})$, provided that $(E_j e_{ij})/(H(d_{ij})) > (\delta_{ij})/(\kappa_{ij})$. This determination will be detailed in Section V. Next, the channel access profitability is introduced. ■

B. Channel Access Profitability

Here, we define the *channel access profitability* that enables each sensor node to regulate its channel access persistence to provide reliable sensor–actor communication. The aim of channel access profitability is to allow each sensor node to obtain a sufficient level of packet transmission rate by regulating its channel access persistence. Suppose that sensor node i transmits its data frames at the beginning of each time slot with a fixed probability p_i. Let us also assume that T_k is the time elapsed between successful transmissions of $(k-1)$th and kth frames. T_k values are drawn from the same probability distribution and are assumed to be independent of one another.

The sequence of T_k can be modeled as interarrival times of a homogeneous Poisson process with the exponential density function $f_T(T) = \lambda e^{-\lambda T}$, where λ is the encounter rate of sensor node i with an available slot. Using the sequence of measured T_k, $k \in \mathcal{Z}^+$, it is possible for a sensor node to obtain an unbiased and efficient maximum-likelihood estimate of λ, i.e., $\widehat{\lambda}$, as follows [15]:

$$\widehat{\lambda} = \frac{1}{\frac{1}{B}\sum_{i=1}^{B} T_i}. \tag{15}$$

Since the duration of a time slot is assumed to be on the scale of microseconds, $\widehat{\lambda}$ will be sufficiently large, and the homogeneous Poisson distribution can be approximated as a normal distribution given as $\mathcal{N}(\widehat{\lambda}, \widehat{\lambda})$. Hence, the random variable that characterizes the interarrival times reduces a normally distributed random variable, i.e., $\mathcal{N}(\widehat{\lambda}, \widehat{\lambda})$.

Let us now assume that sensor node i serves s_i source nodes to route their packets toward the actor node and that each source node uses the average reporting frequency rate $f(frames/s)$. Sensor node i receives the average number of fs_i data frames in a second. Therefore, to avoid a possible congestion, sensor node i should achieve a sufficiently high frame transmission rate, i.e., η_i, to provide $fs_i < \eta_i$. In that sense, the channel access profitability of sensor node i, i.e., ϑ_i, can be characterized by the probability that there is no congestion on sensor node i and formulated as follows:

$$\begin{aligned} \vartheta_i &= P(fs_i < \eta_i) \\ &= 1 - \Phi_i(fs_i) \end{aligned} \tag{16}$$

where η_i denotes the successful frame transmission rate of sensor node i and can be characterized by the normal distribution $\mathcal{N}(\widehat{\lambda}, \widehat{\lambda})$. $\Phi_i(.)$ is the cumulative distribution function of $\mathcal{N}(\widehat{\lambda}, \widehat{\lambda})$. Maximization of the channel access profitability, i.e., ϑ_i, also favors the subject of the cross-layer optimization problem given in (8). Using the channel access profitability, BIOX allows each sensor node to keep its channel access profitability above a feasible maximum value. Hence, this enables each sensor node to separately regulate its transmission strategy to prevent possible congestion. The details of this regulation are introduced in Section V.

IV. Bio-Inspired Task Allocation for Actor Nodes

In this section, we introduce an actor task allocation scheme based on a *task allocation profitability* measure. Then, we investigate the stability of the given task allocation mechanism.

A. Task Allocation Profitability

We assume that, initially, M vehicular actor nodes randomly roam in the environment. When an event occurs in the WSAN environment, an actor node called the master actor node is selected to collect the event data generated by source nodes. The master actor node is also selected as the closest actor node to all source nodes. Based on the event information received from the source nodes, the master actor node is assumed to estimate a four-tuple for each of available tasks,[1] i.e., $\mathcal{F}_i = \{b_i, m_i, x_i, y_i\}$ to characterize the properties of task i. b_i denotes the prioritized time[2] for task i and is given as $b_i = o_i G_i(t)$, where o_i is the constant priority of task i, and $G_i(t)$ is the elapsed time at time t since task i first appears in the environment. As soon as task i is performed at time t, $G_i(t)$ is set to zero. m_i is the encounter rate of the master actor node with the task i. x_i and y_i are the coordinates of the estimated location of task i.

The master actor node periodically estimates or updates the four-tuples for each task appearing in the environment, i.e., $\mathcal{F}_i$ $\forall i$, and broadcasts them to other actor nodes. Using the received four-tuples, each actor node decides which task to perform first and sends a request to the master to allocate the decided task. Once the request message is acknowledged by the master, the task is performed by the actor node. To perform a task, the

[1] Here, we assume that each actor node is able to separately estimate a four-tuple for each of available tasks whenever it is selected as a master actor node. However, the estimation of the four-tuples is out of the scope of this paper.

[2] The measure of the prioritized time has been previously used in the existing literature to investigate the stability of networked control systems [16].

vehicular actor node must also come to the close proximity of the task location. Hence, based on the task location, the task allocation time, and its capability in task performance, each actor node estimates its task completion time, i.e., ρ_i. Briefly, ρ_i is a time duration in which the actor node allocates task i and goes to its close proximity and performs it.

Let us assume that K is the set of task IDs that are performed by actor node A and actor node A allocates task i with the probability a_i. Similar to the rate of the gain in the prey model given in (9), for actor node A, the rate of gain in task performance, i.e., J_A, can be expressed as

$$J_A = \frac{\sum\limits_{i \in K} a_i m_i b_i}{\sum\limits_{i \in K} a_i m_i \rho_i}. \tag{17}$$

The probability of performing each task, i.e., $a_i \ \forall i$, is the decision variable for the actor node. Thus, the goal of the actor node is to choose $a_i \ \forall i$ that maximizes J_A. By setting the task allocation profitability, i.e., ψ_i, as $\psi_i = b_i/\rho_i$, BIOX enables each actor node to determine which task should be performed as follows.

1) It first ranks all profitability values as $\psi_1 > \psi_2 > \cdots > \psi_K$. This sorting also changes the ID number of the available tasks in a way that the task having the highest task allocation profitability becomes task 1 with ψ_1, and so on.
2) Then, it performs the tasks when it encounters starting with the most profitable one until the task j that satisfies

$$\frac{\sum_{i=1}^{j} m_i b_i}{\sum_{i=1}^{j} m_i \rho_i} > \frac{b_{j+1}}{\rho_{j+1}}. \tag{18}$$

B. Stability of BIOX Task Allocation

Here, the boundedness of time delay, i.e., $G_i(t) \ \forall i$, is deduced to prove the stability of the given task allocation mechanism by the following theorem:

Lemma 1: Task allocation algorithm in BIOX guarantees that any task i is definitely allocated and performed within a delay bound given as

$$\lim_{t \to \infty} G_i(t) < \frac{\rho_{\min} o_{\max} \rho_i}{o_{\max} \rho_i - o_i \rho_{\min}} + \rho_{\max} \tag{19}$$

where $o_{\max}$ is the maximum of the priority values, i.e., $o_i < o_{\max} \ \forall i$, and $\rho_{\min}$ and $\rho_{\max}$ are the minimum and maximum of the task completion time values, i.e., $\rho_{\min} < \rho_i < \rho_{\max} \ \forall i$.

Proof: Assume that, at time t, task i has not been performed during τ units of time, and all of other tasks are performed at least once in this duration. Hence, at time t, task selection profitability of task i can be given as

$$\psi_i = \frac{G_i(t) o_i}{\rho_i} = \frac{\tau o_i}{\rho_i}. \tag{20}$$

Suppose also that task k has the maximum possible profitability, i.e., ψ_k, at time t. Since task k has been performed at least once before time t, the possible maximum value for $G_k(t)$ can be given as $G_k(t) = \tau - \rho_{\min}$. Task k may also have the maximum priority and the minimum task performing time as $o_k = o_{\max}$ and $\rho_k = \rho_{\min}$, respectively. Hence, substituting $G_k(t) = \tau - \rho_{\min}$, $o_k = o_{\max}$, and $\rho_k = \rho_{\min}$, the maximum possible ψ_k can be given as

$$\psi_k = \frac{(\tau - \rho_{\min}) o_{\max}}{\rho_{\min}}. \tag{21}$$

At time t, to guarantee that task i is performed, $\psi_i > \psi_k$ has to be satisfied, which yields

$$\tau < \frac{\rho_{\min} o_{\max} \rho_i}{o_{\max} \rho_i - o_i \rho_{\min}}. \tag{22}$$

Task i is definitely allocated within the bound in (22). After the allocation, it is also performed within a time duration that is bounded by $\rho_{\max}$. Hence, task i is definitely allocated and performed within a delay bound, i.e.,

$$\lim_{t \to \infty} G_i(t) < \frac{\rho_{\min} o_{\max} \rho_i}{o_{\max} \rho_i - o_i \rho_{\min}} + \rho_{\max}. \tag{23}$$

■

Next, we introduce the BIOX protocol operation.

V. Bio-Inspired Cross-Layer Protocol Operation

In this section, we introduce the next-hop selection and channel access operation of BIOX.

A. Next-Hop Selection

BIOX enables each sensor node to select its next hop node by means of the next-hop selection profitability, i.e., θ_{ij}, given in (10). For the computation of $\theta_{ij} \ \forall j$, sensor node i needs to find $H(d_{ij})$, e_{ij}, and $E_j \ \forall j$ for all of its neighbors toward the master actor node. Here, we assume that each sensor node foreknows its own location, as well as the location of its neighbors by means of an existing localization technique[3] [10]. Hence, it can compute all Euclidean distance to its neighbors and corresponding effective distances, i.e., d_{ij}, $e_{ij} \ \forall j$, and also computes $H(d_{ij}) \ \forall j$. Each sensor node periodically measures and broadcasts its residual energy to all of its neighbors. Therefore, each sensor node i also knows the residual energy level of its neighbors, i.e., $E_j \ \forall j$.

Substituting $H(d_{ij})$, e_{ij}, and E_j into (10), each sensor node i determines $\theta_{ij} \ \forall j$ and establishes its next-hop selection set U_i including all IDs of its possible next hops. Then, using U_i, sensor node i selects its next hop node as a sensor node providing the maximum next-hop selection profitability, i.e., the next hop of sensor node i is sensor node j such that $\{j | \ \forall k \in U_i : \theta_{ik} < \theta_{ij}\}$.

B. Channel Access and Rate Control

After the selection of its next hop, each sensor node computes its channel access profitability, i.e., ϑ_i in (16), to select its transmission probability p_i. For the computation of ϑ_i, sensor node i periodically estimates the arrival rate of its successful

[3]The details of the localization procedure are beyond the scope of this paper.

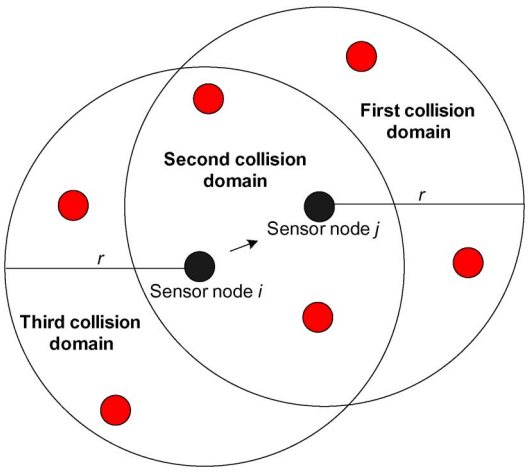

Fig. 2. Collision domains for the link between sensor nodes i and j.

transmissions using the maximum likelihood estimation mechanism given in (15). In one second, sensor node i records time intervals between successful packet transmissions, i.e., $T_k \ \forall k$. At the end of each second, it computes the estimation of the arrival rate of the successful transmissions, i.e., $\widehat{\lambda}$, using (15). Based on the cumulative distribution function of the normal distribution $\mathcal{N}(\widehat{\lambda}, \widehat{\lambda})$, i.e., $\Phi(.)$, sensor node i computes its channel access profitability as $\vartheta_i = 1 - \Phi(fs_i)$.

Each sensor node i regulates its transmission probability in an interval given as $p_{\min} < p_i < p_{\max}$, where $p_{\min}$ and $p_{\max}$ are the minimum and maximum of the transmission probability, respectively. Initially, each sensor node sets its transmission probability as $p_{\min}$ and starts to transmit to its next hop. For a successful transmission of sensor node i, there must be no other transmission in the first, second, and third collision domains, as shown in Fig. 2. Assume that there are g active sensor nodes that transmit with transmission probability p in the first, second, and third collision domains. Therefore, the probability of a successful transmission of sensor node i, i.e., R_i, can be given as

$$R_i = p(1-p)^{g-1}. \tag{24}$$

To find the optimal p that makes R_i maximum

$$\frac{\partial R_i}{\partial p} = (1-p)^{g-1} - (g-1)p(1-p)^{g-2} = 0. \tag{25}$$

This yields the optimal p, i.e., $\overline{p}$, as $\overline{p} = 1/g$. To compute $\overline{p}$, each sensor node i first discovers the number of active sensor nodes in its collision domain, i.e., g. To this end, each active sensor node sends a message to all of its neighbors to notice that it is an active sensor node. This enables each sensor node to discover the number of active sensor nodes g in its collision domains. Then, it sets $p_{\max}$ as $p_{\max} = \overline{p} = 1/g$. Furthermore, $p_{\min}$ is set to a sufficiently low value within the interval [0, 1]. In the simulation experiments, $p_{\min}$ is selected as $p_{\min} = 0.05$. BIOX enables each sensor node to periodically update its transmission probability starting with $p_{\min}$. The aim of this update is to keep the channel access profitability ϑ_i above a predefined threshold value,[4] i.e., $\widetilde{\vartheta}$. The transmission probability update strategy of BIOX is given here.

1) If sensor node i finds ϑ_i as $\vartheta_i < \widetilde{\vartheta}$ and $p_i < p_{\max}$, it updates p_i as $p_i = p_i + \zeta$, where ζ is a small positive constant.
2) If sensor node i finds ϑ_i as $\vartheta_i \geq \widetilde{\vartheta}$, it does not change the current value of p_i.

Based on the updated transmission probability, for the access to the channel, each sensor node generates a uniformly distributed random number h from the interval [0, 1] at the beginning of each time slot. If $p_i > h$, sensor node i transmits to its next hop at the beginning of current slot. Otherwise, sensor node i does not make any transmission during current time slot.

For a successful delivery from sensor node i to sensor node j, there must be no other transmission in the first, second, and third collision domains, as shown in Fig. 2. After a successful delivery, the ACK frame that sensor node j transmits to sensor node i can still collide with the possible ACK frames that are transmitted by the sensor nodes in the first collision domain. For example, assume that, in the first, second, and third collision domains, there is no other transmission, except sensor node i. Assume also that, in the first collision domain, at least one sensor node receives a frame from the outside of the collision domains. In this case, sensor node i successfully delivers a frame to sensor node j. However, if the sensor node in the first collision domain also succeeds to receive a data frame from outside of the collision domains, the ACK frame of sensor node j and this sensor node can collide, and current transmission attempts become unsuccessful.

To mitigate the probability of ACK collision, BIOX allows each sensor node j to send multiple ACKs in the ACK transmission interval for each of the successfully received frames as follows.

1) During the frame transmission interval, sensor node i transmits a data frame to sensor node j with probability p_i. Sensor node i also listens to the channel on whether or not the transmitted data frame has collided.
2) If the transmitted frame has collided, it is retransmitted with probability p_i.
3) If sensor node i successfully delivers a packet to sensor j within the frame transmission interval of a slot, sensor node j immediately sends an ACK frame for this frame in the ACK transmission interval of the slot. ACK frame

TABLE I
SIMULATION PARAMETERS

Number of sensor nodes (N)	100
Environment size	$100 \times 100m - 200 \times 200m$
Transmission range of sensor nodes (r)	$20m$
Queue Size of Sensor Nodes	15KBytes
Number of Actor Nodes (M)	2-8
Number of Source Nodes	80
Frame Length	30 $Bytes$
ACK Frame	5 $Bytes$
Slot Duration	0.001 s

[4]This threshold called as $\widetilde{\vartheta}$ is set as 0.9 in the simulation experiments of this paper.

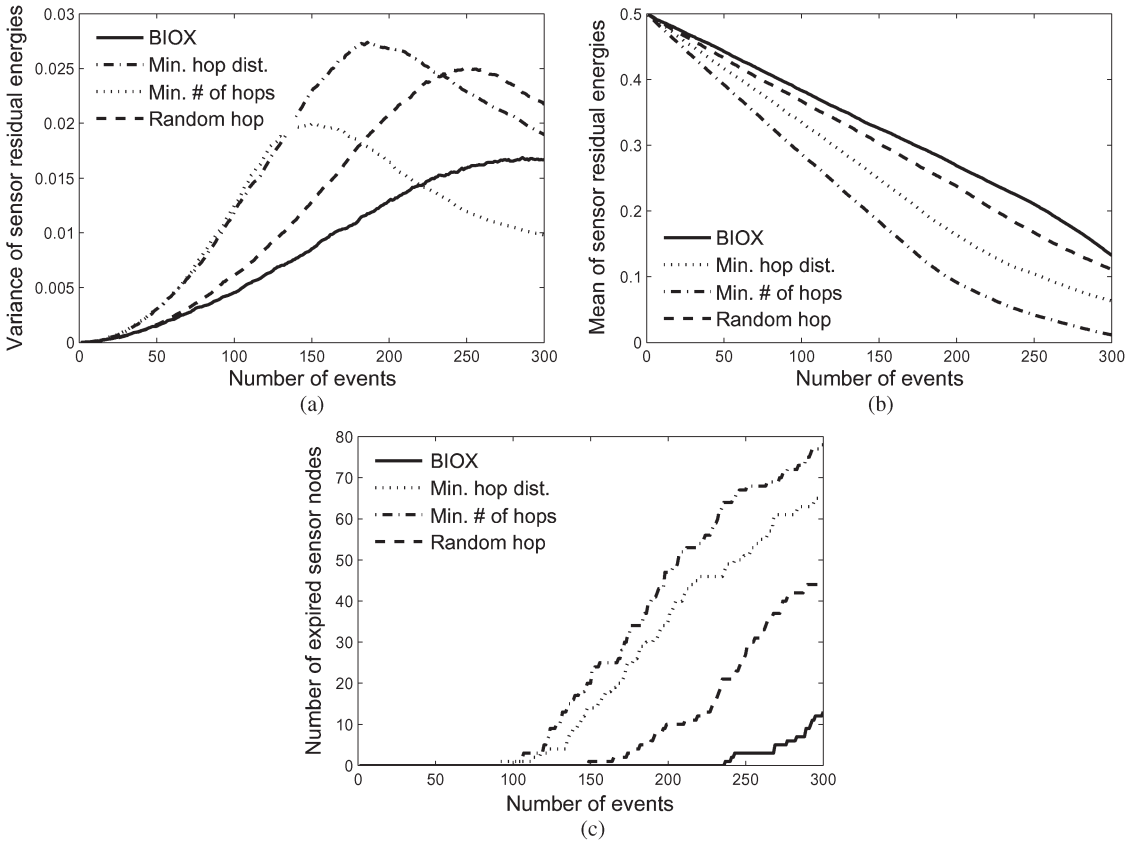

Fig. 3. (a) Variance of sensor residual energies with increasing number of events. (b) Mean of sensor residual energies with increasing number of events. (c) Number of expired nodes with increasing number of events.

includes the IDs of all frames previously received within a fixed time interval.

4) This mitigates the probability of ACK collision in a way that sensor node i can eventually receive an ACK frame including ID number of successfully delivered data frames even if sensor node i did not previously receive an ACK frame belonging to the data frame that is successfully delivered.

Eventually, using next-hop selection and channel access profitability, BIOX allows sensor nodes to estimate and adapt their communication parameters to provide energy-efficient and reliable sensor–actor communication in WSAN.

VI. Performance Evaluation

In this section, we present the performance results of BIOX protocol. For the performance experiments, we develop a simulation environment using MATLAB. The parameters used in the performance analysis are given in Table I.

A. Energy Conservation

To show the BIOX performance on energy conservation, we investigate how the next-hop selection profitability can prolong the network lifetime. When an event occurs, 80 source nodes closest to the event source act as source node and generate data traffic with reporting frequency rate of 40 frame/s. Events are consecutively generated in the different locations of the environment, and each event continues over 1 min.

In Fig. 3(a), the variance of sensor residual energies is shown according to an increasing number of events, and we compare the change in the variance with three fundamental next-hop selection approaches. These approaches provide minimum hop distance, minimum number of hops, and random hop with the same uniform probability. BIOX maintains the variance of sensor residual energies at the minimum level and significantly outperforms the three fundamental approaches. This manifests that BIOX enables sensor nodes to provide balanced energy consumption throughout the network. BIOX also minimizes the total energy consumption throughout the network. This can be easily seen in Fig. 3(b) by observing the mean of sensor residual energies. In Fig. 3(c), the number of expired nodes is shown with an increasing number of consecutive events. BIOX outperforms the minimum hop distance and the minimum number of hop-based approaches by nearly 150% and the random hop-based approach by 75% improvement in network lifetime. Hence, this reveals that BIOX significantly maximizes the network lifetime.

B. Timely and Reliable Sensor–Actor Communication

In this section, we observe the packet delivery ratio, i.e., the ratio of the number of packets delivered to the actors to the total number of transmitted packets by source nodes. In Fig. 4(a), the packet delivery ratio is shown with time for the different numbers of source nodes (n). While n increases, the packet delivery ratio decreases. However, BIOX enables each sensor node to achieve to prevent possible congestion and to eventually

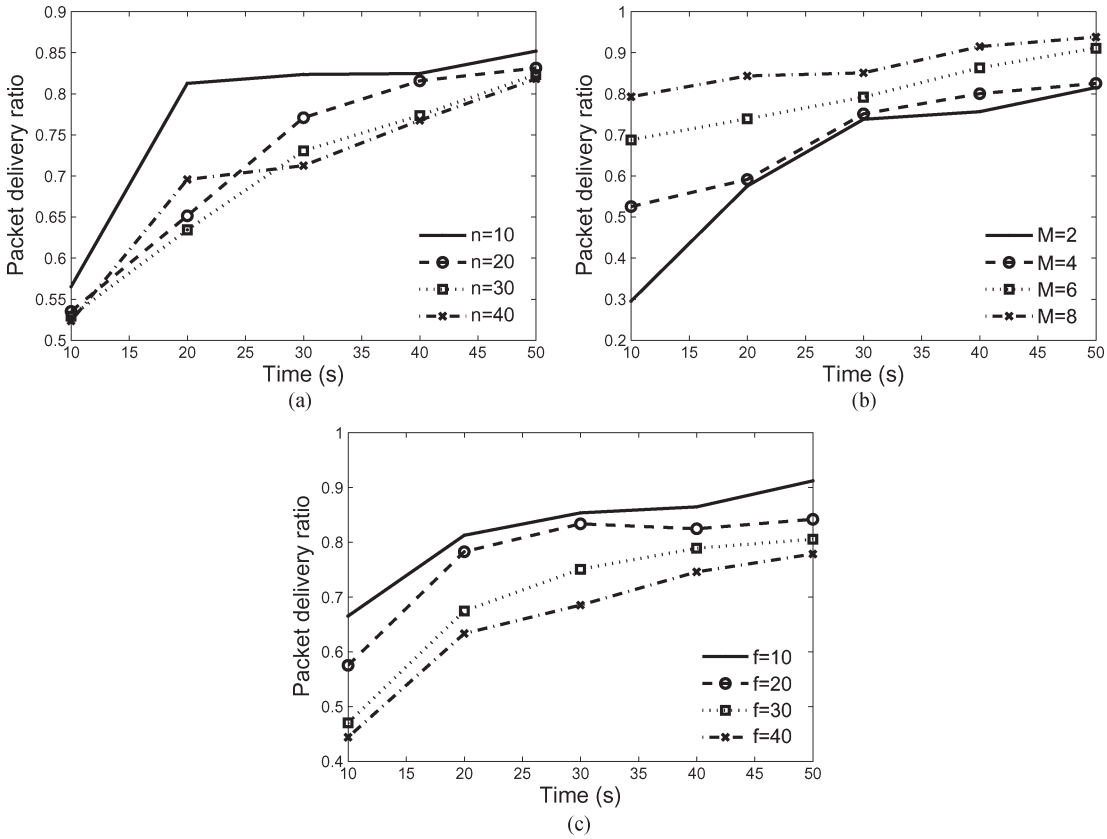

Fig. 4. Packet delivery ratio with time for (a) different numbers of source nodes, (b) different numbers of actor nodes, and (c) different reporting frequencies of source nodes.

TABLE II
COMPARISON OF AVERAGE TASK PERFORMANCE DELAY AND ITS THEORETICAL BOUND GIVEN IN (19)

$\rho_{\min}$	1.5	1.6	1.7	1.8	1.9	2.0	2.1	2.2	2.3	2.4	2.5
$G_i(t)$	2.9317	2.9126	3.0862	3.1294	3.2322	3.3243	3.3207	3.4426	3.4293	3.5261	3.5462
$\overline{G_i(t)}$	5.9464	6.4328	6.7390	7.0952	7.7072	8.0385	8.6083	8.7181	9.3503	10.258	10.9938
$\rho_{\max}$	3.0	2.9	2.8	2.7	2.6	2.5	2.4	2.3	2.2	2.1	2.0
$G_i(t)$	2.9227	2.9142	2.8992	2.8614	2.8208	2.8501	2.7405	2.7112	2.6917	2.6965	2.5206
$\overline{G_i(t)}$	5.9454	6.1074	5.9455	5.9495	5.9114	5.6980	5.9030	5.8371	6.0052	5.8482	5.8910
$o_{\min}$	1.5	1.6	1.7	1.8	1.9	2.0	2.1	2.2	2.3	2.4	2.5
$G_i(t)$	2.9166	2.9231	2.8585	2.8689	2.7713	2.7854	2.7157	2.7263	2.6776	2.6569	2.6813
$\overline{G_i(t)}$	5.9833	6.1608	6.0345	6.0987	6.2792	6.3411	6.5253	6.7544	6.5550	6.7811	6.9354
$o_{\max}$	3.0	2.9	2.8	2.7	2.6	2.5	2.4	2.3	2.2	2.1	2.0
$G_i(t)$	2.8779	2.9213	2.9439	2.8217	2.8937	2.8476	2.7902	2.8056	2.7763	2.7954	2.8193
$\overline{G_i(t)}$	5.9515	5.9881	6.1458	6.3452	6.0813	6.1194	6.2540	6.2275	6.4212	6.5920	6.5088

deliver more than 80% of total packets generated by source nodes.

In Fig. 4(b), the packet delivery ratio is shown with time for the different numbers of actor nodes. As the number of actor nodes increases, the number of hops over the network decreases. This naturally decreases the collision probability over the network, and the BIOX protocol can converge to more than 90% of packet delivery ratio as the number actor nodes increases. Even if two actor nodes are used, BIOX also provides high packet delivery ratio. In Fig. 4(c), the packet delivery ratio is evaluated for f values. As f increases, the average collision probability over the network increases, which clearly decreases the packet delivery ratio. However, BIOX provides high packet delivery ratio near 70% of the packet delivery ratio, even if $f = 40$ is used by the source nodes.

C. Efficient Task Allocation

In Table II, the average task performance delay, i.e., the average time elapsed until a task is accomplished, is compared to the theoretical delay bound in (19) for the different values of $\rho_{\min}$, $\rho_{\max}$, $o_{\min}$, and $o_{\max}$ with the number of 20 tasks that are consecutively appear and are accomplished by five actor nodes. It is shown that the given theoretical delay bound can be justified by the simulation experiments. The delay and theoretical upper bound increase with $\rho_{\min}$; however, they can be reduced by decreasing $\rho_{\max}$. Furthermore, the task performance delay can also be decreased by reducing $o_{\min}$. Conversely, decreasing $o_{\max}$ slightly affects the task performance delay, which stems from the fact that the difference between $o_{\min}$ and $o_{\max}$ becomes too low such that almost all tasks have the same priority values.

VII. Conclusion

In this paper, inspired by a prey model in foraging theory, we have introduced the BIOX Communication and Coordination Protocol for WSANs. BIOX is a unified algorithm that incorporates medium-access-control, routing, and transport layer functionalities to enable each sensor node to separately select and access its next hop node using the bio-inspired next-hop selection and channel access profitability measures. BIOX also uses the bio-inspired task allocation profitability measure for efficient allocation of the available tasks associated with the event. BIOX provides an optimal performance for the energy-efficient and reliable sensor–actor communication, and task allocation. Due to its fully autonomous operations, BIOX can steadily keep the network in a highly reliable and energy-efficient state. This renders BIOX a robust and energy-efficient protocol for the realization of future WSAN applications.

References

[1] I. F. Akyildiz and I. H. Kasimoglu, "Wireless sensor and actor networks: Research challenges," *Ad Hoc Netw.*, vol. 2, no. 4, pp. 351–367, Oct. 2004.
[2] C. Y. Wan, A. T. Campbell, and L. Krishnamurthy, "PSFQ: A reliable transport protocol for wireless sensor networks," in *Proc. ACM WSNA*, Atlanta, GA, 2002, pp. 1–11.
[3] O. B. Akan and I. F. Akyildiz, "ESRT: Event-to-sink reliable transport in wireless sensor networks," *IEEE/ACM Trans. Netw.*, vol. 13, no. 5, pp. 1003–1016, Oct. 2005.
[4] C. Y. Wan, S. B. Eisenman, and A. T. Campbell, "CODA: Congestion detection and avoidance in sensor networks," in *Proc. ACM SENSYS*, Los Angeles, CA, 2003, pp. 266–279.
[5] T. Melodia, D. Pompili, C. V. Gungor, and I. F. Akyildiz, "A distributed coordination framework for wireless sensor and actor networks," in *Proc. ACM MOBIHOC*, Urbana-Champaign, IL, 2005, pp. 99–110.
[6] V. C. Gungor, O. B. Akan, and I. F. Akyildiz, "A real-time and reliable transport protocol for wireless sensor and actor networks," *IEEE/ACM Trans. Netw.*, vol. 16, no. 2, pp. 359–370, Apr. 2008.
[7] B. Fan, K. S. Munasinghe, and A. Jamalipour, "A critical observation collection method for sensor networks inspired by behavioral ecology," in *Proc. PIMRC*, Sep. 2010, pp. 1625–1630.
[8] B. Fan, K. S. Munasinghe, and A. Jamalipour, "An ecologically inspired intelligent agent assisted wireless sensor network for data reconstruction," in *Proc. ICC*, May 2010, pp. 1–5.
[9] T. H. Labella and F. Dressler, "A bio-inspired architecture for division of labour in SANETs," *Adv. Biol. Inspired Inf. Syst.*, vol. 69, pp. 211–230, 2007, Springer.
[10] K. Langendoen and N. Reijers, "Distributed localization in wireless sensor networks: A quantitative comparison," *Comput. Netw.*, vol. 43, no. 4, pp. 499–518, Nov. 2003.
[11] W. R. Heinzelman, A. Chandrakasan, and H. Balakrishnan, "An application-specific protocol architecture for wireless microsensor networks," *IEEE Trans. Wireless Commun.*, vol. 1, no. 4, pp. 660–670, Oct. 2002.
[12] D. Stephens and J. Krebs, *Foraging Theory*. Princeton, NJ: Princeton Univ. Press, 1986.
[13] A. Houston and J. McNamara, *Models of Adaptive Behavior*. Cambridge, U.K.: Cambridge Univ. Press, 1999.
[14] K. M. Passino, "Biomimicry of bacterial foraging for distributed optimization," *IEEE Control Syst. Mag.*, vol. 22, no. 3, pp. 52–67, Jun. 2002.
[15] C. W. Therrien, *Discrete Random Signals and Statistical Signal Processing*. Englewood Cliffs, NJ: Prentice–Hall, 1992.
[16] A. E. Gil, K. M. Passino, S. Ganapathy, and A. Sparks, "Cooperative scheduling of tasks for networked uninhabited autonomous vehicles," in *Proc. IEEE Conf. Decision Control*, Dec. 2003, vol. 1, pp. 522–527.

Baris Atakan (M'09) received the B.Sc. and M.Sc. degrees in electrical and electronics engineering from Ankara University and Middle East Technical University, Ankara, Turkey, in 2000 and 2005, respectively, and the Ph.D. degree in electrical and electronics engineering from Koc University, Istanbul, Turkey, in 2011.

He is currently a Postdoctoral Research Fellow with the Broadband and Wireless Networking Laboratory, School of Electrical and Computer Engineering, Georgia Institute of Technology, Atlanta, under the supervision of Prof. I. F. Akyildiz. His current research interests include nanoscale and molecular communication, nanonetworks, and biologically inspired communication protocols for wireless networks.

Ozgur B. Akan (M'00–SM'07) received the Ph.D. degree in electrical and computer engineering from Georgia Institute of Technology, Atlanta, in 2004.

He is currently a Full Professor with the Department of Electrical and Electronics Engineering, Koc University, Istanbul, Turkey, and the Director of the Next-Generation and Wireless Communications Laboratory. He is an Associate Editor for the *International Journal of Communication Systems* (Wiley) and *Nano Communication Networks Journal* (Elsevier). His current research interests are wireless communications, nanoscale and molecular communications, and information theory.

Prof. Akan is an Associate Editor for the IEEE TRANSACTIONS ON VEHICULAR TECHNOLOGY. He is currently the General Co-Chair of ACM MOBICOM 2012 and the IEEE International Workshop on Molecular and Nanoscale Communications 2012, as well as the Technical Program Committee Co-Chair of the IEEE Symposium on Computers and Communications 2012.